Inorg. Chem. **2006**, *45*, 5119–5125

Hydrogen Atom Abstraction by a High-Valent Manganese(V)–Oxo Corrolazine

David E. Lansky and David P. Goldberg*

Department of Chemistry, Johns Hopkins University, 3400 North Charles Street, Baltimore, Maryland 21218

Received March 23, 2006

High-valent metal–oxo complexes are postulated as key intermediates for a wide range of enzymatic and synthetic processes. To gain an understanding of these processes, the reactivity of an isolated, well-characterized Mn^{V}–oxo complex, $(TBP_8Cz)Mn^{V}{\equiv}O$ (**1**), (TBP_8Cz = octakis(*para-tert*-butylphenyl)corrolazinato^{3-}) has been examined. This complex has been shown to oxidize a series of substituted phenols (4-X-2,6-*t*-$Bu_2C_6H_2OH$, X = $C(CH_3)_3$ (**3**), H, Me, OMe, CN), resulting in the production of phenoxyl radicals and the Mn^{III} complex [$(TBP_8Cz)Mn^{III}$] (**2**). Kinetic studies have led to the determination of second-order rate constants for the phenol substrates, which give a Hammett correlation ($(\log k''_X/k''_H)$ vs σ_p^+) with $\rho = -1.26$. A plot of log *k* versus BDE(O–H) also reveals a linear correlation. These data, combined with a KIE of 5.9 for **3**–OD, provide strong evidence for a concerted hydrogen-atom-abstraction mechanism. Substrates with C–H bonds (1,4-cyclohexadiene and 9,10-dihydroanthracene) are also oxidized via H-atom abstraction by **1**, although at a much slower rate. Given the stability of **1**, and in particular its low redox potential, (–0.05 V vs SCE), the observed H atom abstraction ability is surprising. These findings support a hypothesis regarding how certain heme enzymes can perform difficult H-atom abstractions while avoiding the generation of high-valent metal–oxo intermediates with oxidation potentials that would lead to the destruction of the surrounding protein environment.

Introduction

Understanding the principles that govern the reactivity of high-valent metal−oxo species is critical for delineating the mechanisms of action of heme enzymes (e.g., cytochrome P450, peroxidases), as well as related synthetic porphyrin catalysts. For example, a Compound I-type species ((porph)Fe^{v}(O) or ($porph^{+\bullet}$)Fe^{IV}(O)) has been proposed as the reactive intermediate responsible for the initial oxidation of inert hydrocarbons by cytochrome P450, despite the lack of direct evidence for such a species. Debate still continues over the details of the P450 mechanism, although a hydrogen-atom abstraction by the high-valent metal−oxo intermediate may be the most likely first step.[1,2] The study of high-valent iron−oxo porphyrin model compounds has contributed significantly to understanding the P450 mechanism, and the examination of the analogous high-valent manganese−oxo species has also helped in this regard by contributing to the general understanding of high-valent porphyrin/heme chemistry.[3,4] In addition, high-valent Mn(O) species have been postulated as the key intermediates in a wide range of synthetic porphyrin,[4−8] as well as non-porphyrin (e.g., salen),[9−11] Mn-catalyzed oxidation reactions. The $Mn^{V}{\equiv}O$ unit is also a potentially important intermediate in photosystem II, particularly in regard to net hydrogen-atom transfer processes with a nearby tyrosyl radical.[12,13]

* To whom correspondence should be addressed. E-mail: dpg@jhu.edu.

(1) Meunier, B.; de Visser, S. P.; Shaik, S. *Chem. Rev.* **2004**, *104*, 3947−3980.
(2) Sono, M.; Roach, M. P.; Coulter, E. D.; Dawson, J. H. *Chem. Rev.* **1996**, *96*, 2841−2887.
(3) Fujii, H. *Coord. Chem. Rev.* **2002**, *226*, 51−60.
(4) McLain, J. L.; Lee, J.; Groves, J. T., Biomimetic Oxygenations Related to Cytochrome P450: Metal-Oxo and Metal-Peroxo Intermediates. In *Biomimetic Oxidations Catalyzed by Transition Metal Complexes*; Meunier, B., Ed.; Imperial College Press: London, 2000; pp 91−169.
(5) Battioni, P.; Renaud, J. P.; Bartoli, J. F.; Reinaartiles, M.; Fort, M.; Mansuy, D. *J. Am. Chem. Soc.* **1988**, *110*, 8462−8470.
(6) Bernadou, J.; Fabiano, A.-S.; Robert, A.; Meunier, B. *J. Am. Chem. Soc.* **1994**, *116*, 9375−9376.
(7) Jin, N.; Bourassa, J. L.; Tizio, S. C.; Groves, J. T. *Angew. Chem., Int. Ed.* **2000**, *39*, 3849−3851.
(8) Jin, N.; Groves, J. T., *J. Am. Chem. Soc.* **1999**, *121*, 2923−2924.
(9) Palucki, M.; Finney, N. S.; Pospisil, P. J.; Güler, M. L.; Ishida, T.; Jacobsen, E. N., *J. Am. Chem. Soc.* **1998**, *120*, 948−954.
(10) Khavrutskii, I. V.; Musaev, D. G.; Morokuma, K. *Inorg. Chem.* **2005**, *44*, 306−315.
(11) Adam, W.; Roschmann, K. J.; Saha-Moller, C. R.; Seebach, D. *J. Am. Chem. Soc.* **2002**, *124*, 5068−5073.

10.1021/ic060491+ CCC: $33.50
Published on Web 05/26/2006

The generation and characterization of high-valent Mn−oxo complexes has been a difficult challenge for the synthetic chemist. Only recently have researchers been able to spectroscopically observe (porphyrinoid)Mn^{V}≡O species.[8,14−18] We have recently described the synthesis of an Mn^{v}≡O complex that was stable enough for isolation and characterization at room temperature, taking advantage of a new corrolazine ligand that we have developed, TBP_8Cz, (TBP_8Cz = octakis(*para*-*tert*-butylphenyl)corrolazinato^{3-}).[19,20] The stability of [(TBP_8Cz)Mn^{V}(O)] (**1**) is in part due to the 3− charge provided by the corrolazine, as opposed to the 2− charge of a conventional porphyrin, which helps to offset the hight-valent state of the manganese(V) ion. The analogous corroles, which carry the same charge when fully deprotonated, are also known to stabilize unusually high-valent transition metals, including Mn^{V}.[14,16,21]

The increased stability of **1** is a distinct advantage for determining its physical properties and obtaining a detailed spectroscopic characterization of this molecule[19] but implies an inherent loss of reactivity toward substrate oxidation. However, we have shown that **1** is competent to oxidize PPh_3 and PhSMe via oxygen-atom-transfer (OAT) to give $OPPh_3$ and PhS(O)Me, respectively, and this reactivity is likely based on the relative bond strengths of the Mn−O bond broken versus the O−P and O−S bonds formed.[22,23] In work presented here, we demonstrate that **1** is capable of another type of oxidation involving hydrogen-atom abstractions from substrates with O−H or C−H bonds. To our knowledge, this is the first demonstration of hydrogen-atom abstraction by an isolated Mn^{V}≡O complex of either porphyrin or non-porphyrin type. As found for the OAT reactions, this reactivity is surprising given the inherent stability of **1**. In particular, the low reduction potential for **1**, −0.05 V vs SCE,[19] suggests that its affinity for an H atom should be weak when one considers the thermodynamics of H-atom abstraction separated into its component steps, i.e., transfer of an electron and proton.[24] Recently, an intriguing rationale was offered on the basis of data for chloroperoxidase (CPO) to explain how high-valent metal−oxo intermediates generated in enzymes such as CPO and P450 are allowed to perform H-atom abstractions despite redox potentials that need to be low enough to avoid oxidative destruction of the surrounding protein.[25] The direct assessment of the reactivity of **1** described here provides concrete experimental evidence that high-valent metal−oxo porphyrinoid complexes are capable of H-atom abstraction despite weak oxidizing power.

II. Experimental Section

Materials. Manganese(V)−oxo 2,3,7,8,12,13,17,18-octakis-(4-*tert*-butylphenyl) corrolazine (TBP_8Cz)Mn^{V}(O) (**1**) and manganese(III) 2,3,7,8,12,13,17,18-octakis-(4-*tert*-butylphenyl) corrolazine (**2**) were synthesized according to published procedures.[19] Methylene chloride was distilled over CaH_2 under an inert atmosphere. Anhydrous benzene and toluene were used as received from Aldrich. 2,4,6-Tri-*tert*-butylphenol (**3**), 2,6-di-*tert*-butylphenol, 2,6-di-*tert*-butyl-4-methylphenol, 2,6-di-*tert*-butyl-4-methoxyphenol, 3,5-di-*tert*-butyl-4-hydroxybenzonitrile, 2,4-di-*tert*-butylphenol (**4**), cyclohexadiene (CHD), and dihydroanthracene (DHA) were purchased from Acros in the highest purity and used as received. The coupled product 2,2′-dihydroxy-3,3′,5,5′-tetra-*tert*-butylbiphenyl (**5**) was obtained as a gift from Prof. K. D. Karlin, Department of Chemistry, Johns Hopkins University. Deuterium oxide and dimethyl sulfoxide-d_6 were purchased from Cambridge Isotopes in the highest purity and used as received.

General Instrumentation. UV−vis spectroscopy was performed on a Hewlett-Packard 8452 diode-array spectrophotometer equipped with HPChemstation software. Gas chromatography was performed on an Agilent 6850 gas chromatograph fitted with a DB-5 5% phenylmethyl siloxane capillary column (30 m × 0.32 mm × 0.25 μm) and equipped with a flame-ionization detector (FID) or a Shimadzu GC-17A gas chromatograph outfitted with a DB-5MS column and interfaced with a Shimadzu QP-5050A mass spectrometer. NMR spectra were recorded on a Bruker Avance 400 NMR instrument at 400 MHz (^{1}H). All spectra were recorded in 5-mm o.d. NMR tubes, and chemical shifts were reported as δ values from standard solvent peaks. Electron paramagnetic resonance (EPR) spectra were obtained on a Bruker EMX EPR spectrometer controlled with a Bruker ER 041 X G microwave bridge.

Reaction of (TBP_8Cz)Mn^{V}≡O and 2,4,6-Tri-*tert*-butylphenol for Analysis by EPR Spectroscopy. Under an inert atmosphere, an amount of **1** (5.0 mg, 3.5×10^{-6} mol) and 2,4,6-tri-*tert*-butylphenol (1.0 mg, 3.81×10^{-6} mol) were dissolved in toluene (0.5 mL). The reaction mixture was stirred for 20 min, and the color changed from green to brown, indicating conversion of **1** to **3**. The reaction mixture was then transferred to a 3-mm quartz EPR tube which was sealed and immediately frozen in liquid nitrogen. The EPR samples prepared in this manner were stored at 77 K until EPR spectra were recorded.

Kinetic Studies. Reaction of (TBP_8Cz)Mn^{V}≡O and Phenol Substrates. Kinetic runs for the reaction between **1** and phenol substrates were done under pseudo-first-order conditions with excess substrate. Reactions were monitored by following the decrease in the absorbance of the Q-band peak for **1** at 634 nm. A typical kinetics run is described as follows for substrate **4**, and the same

(12) Yachandra, V. K.; Sauer, K.; Klein, M. P. *Chem. Rev.* **1996**, *96*, 2927−2950.
(13) Yagi, M.; Kaneko, M. *Chem. Rev.* **2001**, *101*, 21−35.
(14) Gross, Z.; Golubkov, G.; Simkhovich, L. *Angew. Chem., Int. Ed.* **2000**, *39*, 4045−4047.
(15) Groves, J. T.; Lee, J.; Marla, S. S. *J. Am. Chem. Soc.* **1997**, *119*, 6269−6273.
(16) Liu, H. Y.; Lai, T. S.; Yeung, L. L.; Chang, C. K. *Org. Lett.* **2003**, *5*, 617−620.
(17) Nam, W.; Kim, I.; Lim, M. H.; Choi, H. J.; Lee, J. S.; Jang, H. G. *Chem. Eur. J.* **2002**, *8*, 2067−2071.
(18) Zhang, R.; Horner, J. H.; Newcomb, M. *J. Am. Chem. Soc.* **2005**, *127*, 6573−6582.
(19) Lansky, D. E.; Mandimutsira, B.; Ramdhanie, B.; Clausén, M.; Penner-Hahn, J.; Zvyagin, S. A.; Telser, J.; Krzystek, J.; Zhan, R. Q.; Ou, Z. P.; Kadish, K. M.; Zakharov, L.; Rheingold, A. L.; Goldberg, D. P. *Inorg. Chem.* **2005**, *44*, 4485−4498.
(20) Mandimutsira, B. S.; Ramdhanie, B.; Todd, R. C.; Wang, H. L.; Zareba, A. A.; Czernuszewicz, R. S.; Goldberg, D. P. *J. Am. Chem. Soc.* **2002**, *124*, 5170−15171.
(21) Eikey, R. A.; Khan, S. I.; Abu-Omar, M. M. *Angew. Chem., Int. Ed.* **2002**, *41*, 3592−3595.
(22) Kerber, W. D.; Goldberg, D. P. *J. Inorg. Biochem.* **2006**, *100*, 838−857.
(23) Wang, S. H. L.; Mandimutsira, B. S.; Todd, R.; Ramdhanie, B.; Fox, J. P.; Goldberg, D. P. *J. Am. Chem. Soc.* **2004**, *126*, 8−19.
(24) Mayer, J. M., Biomimetic Oxygenations Related to Cytochrome P450: Metal-Oxo and Metal-Peroxo Intermediates. In *Biomimetic Oxidations Catalyzed by Transition Metal Complexes*; Meunier, B., Ed. Imperial College Press: London, 2000; pp 1−43.
(25) Green, M. T.; Dawson, J. H.; Gray, H. B. *Science* **2004**, *304*, 1653−1656.

Scheme 1

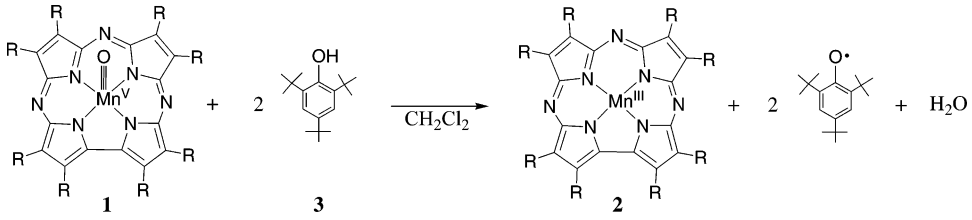

method was employed for all other substrates. An amount of **1** (1.64 × 10^{-7} mol) was dissolved in 10 mL of CH_2Cl_2 in a modified 250-mL round-bottom flask fused to a sidearm valve and a quartz UV−vis cell (cell vol 3 mL). Different amounts of a stock solution of **4** in CH_2Cl_2 (final concentration 0.42−18 mM) were injected by syringe to initiate the reaction. UV−vis spectra were then collected every 5−600 s, depending upon the rate of the reaction. A minimum of four different concentrations were run for each substrate, and pseudo-first-order rate constants (k_{obs}) at each concentration were collected at least twice. The k_{obs} values were obtained by fitting a plot of A_{634nm} versus time to the equation $A_t = A_f - (A_f - A_0)e^{-kt}$. Where A_f = final absorbance and A_0 = initial absorbance at 634 nm. A natural log plot of the same data was linear to at least 3 half-lives in all cases.

Control Experiment To Determine the Stability of (TBP$_8$Cz)-Mn^V≡O. A control experiment was run in which a solution of **1** (2.0 × 10^{-7} mol) in 10 mL of CH_2Cl_2 was monitored at 634 nm (Q-band) to observe any background decay. After 5 days, there was no change in the overall spectrum of **1** (300−800 nm) and there was no change in absorbance at 634 nm.

Synthesis of 2,4,6-(C(CH$_3$)$_3$)−C$_6$H$_2$OD. The phenol **3** (0.13 g, 0.50 mmol) was deprotonated with KH (0.02 g, 0.50 mmol) in 3 mL of DMSO-d_6 under an inert atmosphere for 18 h. An amount of D_2O (5 mL) was then added, causing a white solid to precipitate. This solid was isolated by filtration and dried under vacuum. ^{1}H NMR (400 MHz, $CDCl_3$) indicated complete loss of the phenol proton at 5.02 ppm, >99% deuteration.

Kinetic Studies. **Reaction of (TBP$_8$Cz)Mn^V≡O and C−H Substrates.** Kinetic runs for the reaction between **1** and CHD and DHA were performed in a manner similar to those for the phenol substrates. Reactions were monitored by following the decrease in the absorbance of the Q-band peak for **1** at 634 nm. A typical kinetics run is described as follows for CHD: An amount of **1** (1.11 × 10^{-7} mol) was dissolved in 10 mL of CH_2Cl_2. Different amounts of a stock solution of CHD in CH_2Cl_2 (final concentration 0.85−57 mM) were injected by syringe to initiate the reaction. UV−vis spectra were then collected every 300−1800 s depending upon the concentration of substrate. The data were analyzed and the rate constants were obtained by using the same methods as for the phenol experiments. Good first-order behavior ≥3 half-lives was noted for both CHD and DHA. The second-order rate constants (k") thus obtained were adjusted for the statistical factor arising from the four equivalent, reactive C−H bonds in both substrates and are reported as k" per C−H bond.

Reaction of 1 and 4. Product Analysis by GC-FID and GC-MS. A typical reaction was conducted as follows. Under an argon atmosphere, **1** (6.3 mg, 4.4 × 10^{-3} mmol) was added as a solid to a Schlenk flask and then dissolved in 1.0 mL of a stock solution of **4** (5.23 mM in CH_2Cl_2). The reaction mixture was stirred for 1 h at room temperature, during which time the solution changed from the green color indicative of **1** to the brown color of **2**. Complete conversion of **1** to **2** was then confirmed by UV−vis spectroscopy by sampling an aliquot of the reaction mixture. An amount of octadecane (100 μL) was then added from a stock solution (23.6 mM in CH_2Cl_2) as an internal standard. An aliquot was removed and injected directly onto the GC-FID, and GC traces showed peaks for the coupled product **5** (12.0 min), the remaining starting material **4** (2.9 min), and octadecane (4.9 min). All peaks of interest were identified by comparison of retention times and co-injection with authentic samples. Compounds were quantified by comparison against a known amount of octadecane using a calibration curve consisting of a plot of mole ratio (moles of compound of interest/moles of internal standard) versus area ratio (area of compound of interest/area of internal standard). Calibration curves were prepared by using concentrations in the same range as that observed in the actual reaction mixtures. For identification of unknown peaks, an aliquot of the reaction mixture was directly injected onto the GC-MS. GC-FID and GC-MS conditions: An initial oven temperature of 200 °C was held for 5 min and then raised 10 °C/min for 5 min until a temperature of 250 °C was reached, which was then held for 5 min.

Dependence of the Rate Constants on Temperature for Reaction of 1 and 4. The temperature-dependence of the rate constants were measured in a UV−vis cuvette in which the temperature was controlled by an external continuous-flow water bath. The temperature of the solution was monitored by an Omega HH21 microprocessor thermometer (thermocouple) placed directly in the UV−vis cell. Reaction conditions are the same as described in the Kinetic Studies, except that benzene was selected as a solvent in order to have a wide temperature range. The sample was allowed to equilibrate to the set temperature for 15 min prior to initiating the reaction. The temperature was varied from 293 to 327 K. Activation parameters were obtained from plots of ln(k"/T) versus 1/T according to the Eyring equation.

Results and Discussion

Reaction of (TBP$_8$Cz)Mn^V≡O with 2,4,6-Tri-*tert*-butylphenol. The first indication that the Mn^V−oxo complex **1** was capable of oxidizing phenols came from the reaction with **3**, Scheme 1. This substrate was selected because of its well-known property to give a stable phenoxyl radical after formal H-atom abstraction, which could easily be identified by EPR spectroscopy.[26] The reaction was initially monitored by UV−vis spectroscopy and revealed a smooth conversion of **1** (λ_{max} = 418, 634 nm) to the Mn^{III} complex **2** (λ_{max} = 435, 685 nm), with tight isosbestic behavior (Figure 1). An EPR spectrum of the reaction mixture showed an intense, sharp singlet at g = 2.003 (ΔH = 11 G, room temperature). Both the Mn^V(O) and Mn^{III} complexes are EPR silent, and this spectrum was easily assigned to the stable phenoxyl radical product.[26] The UV−vis and EPR data indicate that the Mn^V−oxo complex oxidizes the phenol **3** via a formal hydrogen-atom abstraction, although there are several possible mechanisms for this process. In addition to a concerted

(26) Altwicker, E. R. *Chem. Rev.* **1967**, *67*, 475−531.

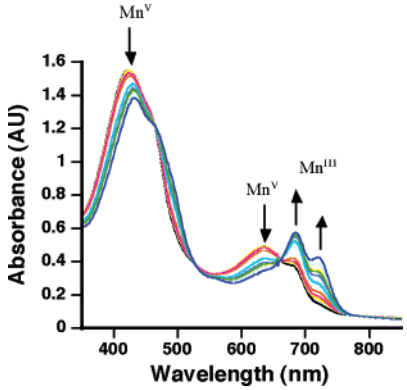

Figure 1. UV−vis spectra of **1** + **3** (100 equiv) in CH_2Cl_2 over 1 h.

Table 1. Second-order Rate Constants for Reaction of **1** with Phenol Substrates in CH_2Cl_2

substrate	k'' ($M^{-1}s^{-1}$)
2,4-*t*-$Bu_2C_6H_3OH$	2.9 ± 0.1
2,4,6-*t*-$Bu_3C_6H_2OH$	$(7.4 \pm 0.7) \times 10^{-2}$
2,4,6-*t*-$Bu_3C_6H_2OD$	$(1.3 \pm 0.1) \times 10^{-2}$
4-OMe-2,6-*t*-$Bu_2C_6H_2OH$	$(4.5 \pm 0.2) \times 10^{-1}$
4-CH_3-2,6-*t*-$Bu_2C_6H_2OH$	$(1.7 \pm 0.1) \times 10^{-2}$
4-H-2,6-*t*-$Bu_2C_6H_2OH$	$(7.8 \pm 0.4) \times 10^{-3}$
4-CN-2,6-*t*-$Bu_2C_6H_2OH$	$(6.0 \pm 0.6) \times 10^{-3}$

H-atom abstraction being the rate-determining step, other possibilities included electron-transfer followed by proton-transfer (ET/PT), or PT followed by ET.

The initial Mn product of this reaction should be an Mn^{IV}−OH species, but no evidence for this species was observed by either UV−vis or EPR, suggesting that it does not accumulate to a measurable extent during the reaction. A reasonable explanation for this observation is that the putative Mn^{IV}−OH intermediate is itself highly reactive and in a second, fast step abstracts a hydrogen atom from a second equivalent of phenol to proceed on to the final Mn^{III} product.[27] The UV−vis spectrum of the final reaction mixture indicated quantitative recovery of the Mn^{III} product, which supports the proposed simple mechanism $Mn^{V}(O)$ + phenol → $Mn^{IV}OH$ + phenol + $PhO^{\bullet}$ → Mn^{III} + $2PhO^{\bullet}$.

Kinetics. To gain a better understanding of the mechanism of phenol oxidation and determine the scope of this reaction, kinetic studies were performed on a series of para-substituted 2,6-di-*tert*-butylphenol substrates (4-X-2,6-*t*-$Bu_2C_6H_2OH$, X = H, Me, OMe, CN) in CH_2Cl_2 at 23 °C. All of these substrates are similar to **3** in that they are known to give stable phenoxyl radicals upon oxidation.[26] The kinetics were followed by the disappearance of **1** (UV−vis) under pseudo-first-order conditions with excess phenol substrate. Isosbestic conversion of **1** to **2** was observed for all substrates, and a representative run is shown in Figure 1 for 2,4,6-tri-*tert*-butylphenol. Good first-order kinetics curves (≥3 half-lives) were obtained in all cases. The first-order rate constants (k_{obs}) were shown to vary linearly with the concentration of each

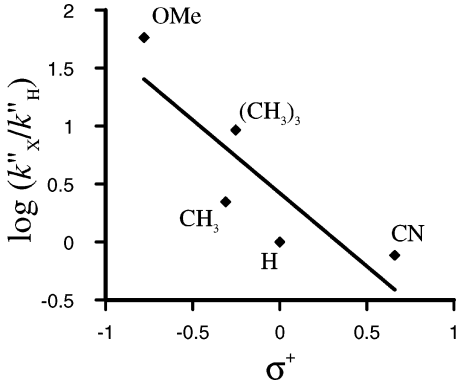

Figure 2. Hammett plot for the reaction of **1** with 4-X-2,6-*t*-$Bu_2C_6H_2OH$ substrates.

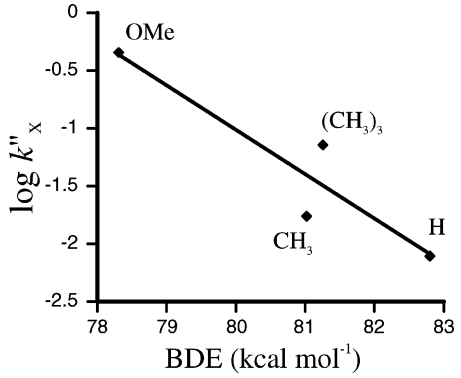

Figure 3. Plot of rate constants versus O−H bond strength for 4-X-2,6-*t*-$Bu_2C_6H_2OH$ substrates.

substrate, indicating a second-order rate law and yielding the second-order rate constants given in Table 1. A Hammett analysis ($\log(k''_X/k''_H) = \rho\sigma_p^+$) of the second-order rate constants thus obtained is shown in Figure 2. A decrease in the relative rates is observed with an increase in the electron-withdrawing nature of the para substituents, giving $\rho = -1.26$. The same negative correlation between σ_p^+ and the rates of H-atom abstraction from YC_6H_4OH by organic radicals is well-known, and can be expected with the formation of an electron-deficient phenoxyl radical.[28−31] The Hammett study points to a concerted hydrogen-atom abstraction as the rate-determining step.

A second informative correlation regarding the mechanism of phenol oxidation comes from a plot of homolytic phenol O−H bond dissociation energies, BDE(O−H), versus $\log(k''_X)$, shown in Figure 3. This plot shows a linear relationship in which the relative rates decrease with increasing O−H bond strength, yielding a slope = −0.39. The BDEs used in this plot were determined by Pedulli and co-workers by an EPR equilibration method, and although their absolute values may be subject to refinement, their relative values should be highly accurate.[32] The para CN substrate

(27) An alternative mechanism would involve the disproportionation of the $Mn^{IV}OH$ species to give **1** and the Mn^{III} product, and **1** is then the only species that oxidizes the phenol substrate. We thank an insightful reviewer for this suggestion. Although we favor the mechanism involving reaction of $Mn^{IV}OH$ with substrate given the large excess of phenol compared to Mn, we cannot rule out this alternative mechanism.

(28) Mahoney, L. R.; DaRooge, M. A. *J. Am. Chem. Soc.* **1970**, *92*, 890−899.
(29) Snelgrove, D. W.; Lusztyk, J.; Banks, J. T.; Mulder, P.; Ingold, K. U. *J. Am. Chem. Soc.* **2001**, *123*, 469−477.
(30) Mulder, P.; Saastad, O. W.; Griller, D. *J. Am. Chem. Soc.* **1988**, *110*, 4090−4092.
(31) Pratt, D. A.; DiLabio, G. A.; Mulder, P.; Ingold, K. U. *Acc. Chem. Res.* **2004**, *37*, 334−40.

was not examined by Pedulli and is therefore not included in Figure 3. A linear relationship between reaction rate and bond strength for C−H bond oxidations by metal complexes such as MnO_4^- has been employed by Mayer as strong evidence for rate-limiting hydrogen-atom abstraction.[24,33] Furthermore, the latter work demonstrated that closed-shell (i.e., nonradical) metal complexes such as MnO_4^- were capable of behaving like open-shell organic radicals (e.g., *tert*-BuOO•) in their ability to abstract H• from substrates. The reactivity of complex **1**, a low-spin d^2 species, provides another example of this phenomenon. Lau and co-workers have also recently shown that the oxidation of a series of phenol substrates by another high-valent metal−oxo complex, $[Ru^{VI}(L)(O)_2]^{2+}$, gives the same linear relationship between rate constants and BDE(O−H), and these workers also concluded an H-atom-abstraction mechanism was operative.[34] The sensitivity of the rate constants to BDE(O−H) represented by the slope in Figure 3 is similar to that found by Mayer for C−H oxidations (−0.4),[35] but intriguingly, is significantly smaller than that found for the phenol reactions measured by Lau (∼ −0.8).[36] Stack and co-workers have observed a weak correlation for C−H oxidations by the lipoxygenase model complex $[Mn^{III}(PY5)(OH)](CF_3SO_3)_2$ (PY5 = 2,6-bis(bis(2-pyridyl)methoxymethane)pyridine) (slope = −0.1), and offer an insightful discussion regarding possible explanations for the relative insensitivity but still conclude H-atom abstraction as the most likely mechanism.[37]

Kinetic Isotope and Steric Effects. Further evidence for an H-atom-abstraction mechanism comes from kinetic isotope and steric effects. Substitution of deuterium for the phenolic proton in **3** led to a significant decrease in rate constant (2,4,6-*t*-$Bu_3C_6H_2OD$, 0.0125 ± 0.0014 M^{-1} s^{-1}; 2,4,6-*t*-$Bu_3C_6H_2OH$, 0.074 ± 0.007 M^{-1} s^{-1}). The resulting KIE (k_H/k_D) of 5.9 provides compelling evidence that the rate-determining step involves O−H bond cleavage, as expected for H-atom transfer. In addition, the effect of decreasing steric congestion near the O−H group was tested by reacting **4** with **1**, which gives a dimerized biphenol product after oxidation (vide infra). A rate constant of $k'' = 2.9 \pm 0.1$ M^{-1} s^{-1} for DTBP was measured, which is nearly 40 times faster than that for TTBP. This large steric effect is in concert with O−H bond cleavage being involved in the rate-determining step.

The mechanistic choices besides H-atom abstraction are shown in Scheme 2: electron transfer **I** followed by proton transfer **II** (ET/PT), or the reverse (PT/ET; **III/IV**), with the PT step in each case being rate-limiting in order to agree with the observed KIE and steric effect. The $E_{1/2}$ for the $[(Cz)Mn^{V}{=}O]/[(Cz)Mn^{IV}{=}O]^-$ couple (−0.05 V in CH_2Cl_2 vs SCE) measured previously[19] is much lower than phenol

Scheme 2

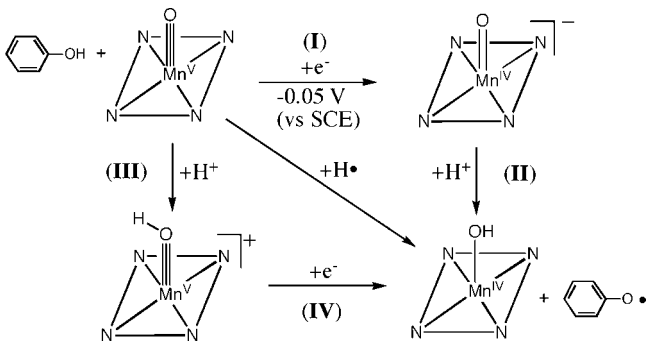

oxidations[38] (e.g., 4-X-C_6H_4OH = 1.2−2.2 V vs SCE), effectively excluding a fast ET event followed by slow PT. The choice of a PT/ET mechanism is more difficult to eliminate. However, it is unlikely that the Mn^V−oxo complex is basic enough to deprotonate the phenol substrates. Additionally, if this were the mechanism, one would expect an opposite correlation of k'' with σ^+, since the phenol pK_a is expected to decrease with σ^+, which in turn should cause an increase in k''. All of the data point to a mechanism that involves concerted H-atom abstraction by the Mn^V−oxo complex.

The observed reactivity for **1** implies that H-atom transfer from the phenols to **1** is thermodynamically favored, which indicates that the BDE for the O−H bond formed in the putative $[(Cz)Mn^{IV}(OH)]$ should be similar to or greater than the O−H bond being broken in the phenol.[24,33] Therefore, a rough estimate for BDE(O−H) in $[(Cz)Mn^{IV}(OH)]$ is ∼80 kcal/mol. This BDE is related to the redox potential ($E_{1/2}$) and pK_a associated with steps **I** and **II** in Scheme 2 through eq 1 (assuming the entropies of **1** and $[(Cz)Mn^{IV}(OH)]$ are equal):

$$\mathrm{BDE} = 23.06E_{1/2} + 1.37\mathrm{p}K_a + C \qquad (1)$$

where C is a constant that accounts for the thermodynamic properties of the hydrogen atom.[24,33,38] A C value of 59.5 kcal/mol was reported for CH_3CN,[24] and although the $E_{1/2}$ for **1** cannot be measured directly in CH_3CN due to a lack of solubility, it does not vary much with solvent (e.g., CH_2Cl_2 (−0.05 V), PhCN (0.02 V), and pyridine (0.03 V)), and therefore, it is reasonable to assume a similar value should hold for CH_3CN. Solving this equation for the pK_a by using a BDE of 80 kcal/mol gives a pK_a = 22 for $[(Cz)Mn^{IV}(OH)]$! Although the true value of this pK_a may vary significantly because of the uncertainty in BDE(O−H) for $Mn^{IV}OH$, this method provides a reasonable estimate of a lower limit for the pK_a since the BDE for $[(Cz)Mn^{IV}(OH)]$ cannot be dramatically lower than ∼80 kcal/mol. If a BDE value of 70 kcal/mol is used, a pK_a of 15 would be obtained, which is still highly basic. These calculations afford some insight into the origins of the reactivity of **1** toward H-atom abstraction. The weak one-electron oxidizing power of **1** reflected in the $E_{1/2}$ value of step **I** may be balanced by the high basicity of $[(Cz)Mn^{IV}(O)]^-$ (pK_a of step **II**), making **1**

(32) Lucarini, M.; Pedrielli, P.; Pedulli, G. F. *J. Org. Chem.* **1996**, *61*, 9259−9263.
(33) Mayer, J. M. *Acc. Chem. Res.* **1998**, *31*, 441−450.
(34) Yiu, D. T. Y.; Lee, M. F. W.; Lam, W. W. Y.; Lau, T. C. *Inorg. Chem.* **2003**, *42*, 1225−1232.
(35) Gardner, K. A.; Kuehnert, L. L.; Mayer, J. M. *Inorg. Chem.* **1997**, *36*, 2069−2078.
(36) Estimated from the slope of the plot in Figure 6b of ref 32.
(37) Goldsmith, C. R.; Cole, A. P.; Stack, T. D. P. *J. Am. Chem. Soc.* **2005**, *127*, 9904−9912.
(38) Bordwell, F. G.; Cheng, J. P. *J. Am. Chem. Soc.* **1991**, *113*, 1736−1743.

Scheme 3

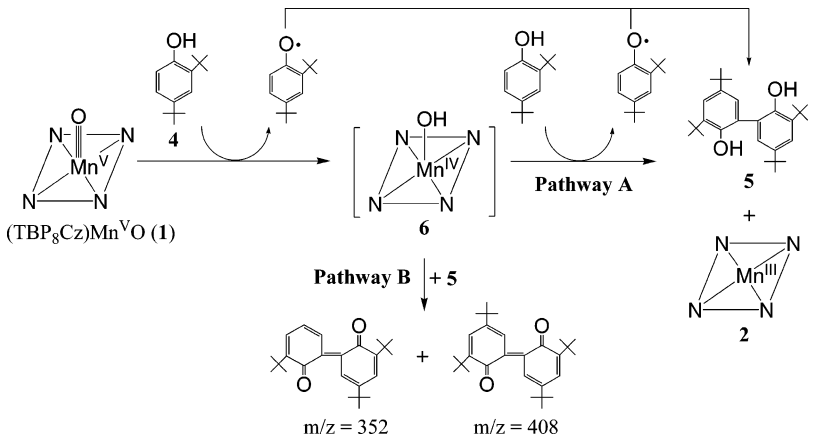

thermodynamically competent to abstract a hydrogen atom from phenol substrates.[39] The high basicity of $[(Cz)Mn^{IV}(O)]^-$ can be rationalized by its overall negative charge, arising from the "extra" negative charge provided by the Cz ligand.

Reaction of $(TBP_8Cz)Mn^V{\equiv}O$ with 4. Reaction with the 2,4-di-*tert*-butyl-substituted phenol **4** was examined because it provided the opportunity to quantitatively assess the organic products formed after oxidation by **1**. Reaction between **1** and **4** in a molar ratio of 1:2.3 in CH_2Cl_2 at 25 °C for 1 h led to the clean formation of the dimer (**5**) in 80% yield, with 15% unreacted **4** remaining (Scheme 3). Monitoring the same reaction by UV−vis spectroscopy revealed that **1** was smoothly converted to the Mn^{III} complex **2**, as seen for the 2,4,6-trisubstituted phenols. Formation of the dimer **5** is expected from a net reaction where 2 equiv of phenol are oxidized by one Mn^V−oxo complex to give the dimer **5** and Mn^{III} complex **2** (Pathway A). Possible intermediates in this pathway are the phenoxyl radical and the putative $Mn^{IV}OH$ (**6**) complex. To see if the $Mn^{IV}OH$ intermediate could be directly observed, we decided to test this reaction under conditions where the phenol was added in limiting amounts, i.e., less than 2 equiv per Mn. Surprisingly, although this variation in stoichiometry did not lead to spectroscopic observation of the $Mn^{IV}(OH)$ species, it caused a dramatic change in product distribution. When **1** and **4** were reacted in a stoichiometry of 1:1, the yield of **5** was only 39% (GC-FID, based on **4**), and when the stoichiometry was changed to 1:0.5, the dimer **5** was not detected at all. In both of these cases, there was <5% of **4** remaining at the end of the reaction. These data indicated that other unidentified oxidation products besides **5** were forming under conditions of limiting amounts of **4**.

Analysis of the latter reactions by GC-MS revealed two new peaks with molecular weights of 352 and 408, which correspond to structures of further oxidation products of **5** (Scheme 3). The mechanism shown in Pathway B of Scheme 3 is proposed to account for these observations. We suggest that, under limiting amounts of phenol, the postulated intermediate **6** reacts with the dimer **5** that is initially formed, leading to the over-oxidized products observed by GC-MS and accounting for the loss of **5**. In other words, the relative rates of Pathway A versus Pathway B determine the product distributions; Pathway A is retarded when limiting amounts of phenol are used, and Pathway B becomes significant. If this scheme is correct, it suggests that the $Mn^{IV}OH$ species is a highly reactive oxidant in its own right. Control reactions between **1** and **5** under pseudo-first-order conditions (large excess of **5**) proceed far too slowly ($k'' = 5.9 \times 10^{-3}$ M^{-1} s^{-1}) to account for the reactivity observed in the cases of limiting amounts of substrate.

There is some limited information regarding the activation parameters for H-atom abstraction from **4** by other metal complexes, and therefore we decided to obtain activation parameters for the reaction of **1** with **4** for comparison. Activation parameters were measured in benzene because this solvent allows for a wider temperature range than CH_2Cl_2 (293−327 K). The parameters thus obtained are $\Delta H^{\ddagger} = 6.3 \pm 1.4$ kcal/mol and $\Delta S^{\ddagger} = -35.6 \pm 2.3$ cal/K·mol. In comparison, the copper^{III} complex $[Cu(H_{-3}Aib_3)]$ (Aib = tri-α-aminoisobutyric acid) reacts with **4** following a second-order rate law to give $\Delta H^{\ddagger} = 8.3 \pm 1.1$ kcal/mol and $\Delta S^{\ddagger} = -27 \pm 3$ cal/K·mol,[40] and the ruthenium^{VI} complex $[Ru(L)(O)_2]^{2+}$ gives $\Delta H^{\ddagger} = 11.3 \pm 0.8$ kcal/mol and $\Delta S^{\ddagger} = -14 \pm 2$ cal/K·mol.[34] There is good agreement between **1** and these other complexes regarding the activation parameters for H-atom abstraction from **4**.

Oxidation of C−H Bonds. We speculated that C−H bonds with similar or weaker bond strengths (BDE(C−H)) to the phenols should also be reactive toward **1**. The C−H substrates cyclohexadiene (CHD) and dihydroanthracene (DHA) were chosen because their bond strengths are 75 ± 4[41] and 78 ± 2 kcal/mol,[38] respectively, which are similar to the phenol O−H bond strengths. Both of these substrates were observed to react with **1** in CH_2Cl_2 at room temperature by UV−vis spectroscopy, causing the smooth decay of **1** into **2**. Good first-order kinetics were observed with these substrates, and second-order rate constants were determined (normalized per reactive C−H bond): k''(CHD) = 3.32 ±

(39) For an example of hydrogen-atom abstraction by an iron(III) complex with a similarly low redox potential, see Roth, J. P.; Mayer, J. M. *Inorg. Chem.* **1999**, *38*, 2760−2761.

(40) Lockwood, M. A.; Blubaugh, T. J.; Collier, A. M.; Lovell, S.; Mayer, J. M. *Angew. Chem., Int. Ed.* **1999**, *38*, 225−227.

(41) Laarhoven, L. J. J.; Mulder, P.; Wayner, D. D. M. *Acc. Chem. Res.* **1999**, *32*, 342−349.

0.12×10^{-5} M^{-1} s^{-1} and k''(DHA) $= 1.76 \pm 0.48 \times 10^{-5}$ M^{-1} s^{-1}. Although these results demonstrate that the Mn^{V}−oxo complex is capable of oxidizing these C−H substrates, these reactions are obviously much slower than those of the phenol substrates. In fact, this dramatic decrease in rate constants on going from O−H to C−H bonds was anticipated on the basis of previous observations of H-atom abstractions by metal complexes.[40]

Conclusions

We have shown that the Mn^{V}−oxo complex **1** oxidizes both O−H and C−H bonds with similar BDEs. The most reasonable mechanism for these oxidations is a concerted H-atom abstraction by the Mn^{V}−oxo complex. This mechanism implies the formation of a transient $Mn^{IV}OH$ species after the rate-determining step, but this intermediate is not detectable, and only the stable Mn^{III} complex is detected as the final product.

How is the Mn^{V}−oxo complex reactive toward H-atom abstraction despite it being stable enough for isolation at room temperature? We suggest that a high affinity for the proton (Step **II** in Scheme 2) by the reduced $[(Cz)Mn^{IV}(O)]^{-}$ may account for much of the driving force for these reactions. Although high-valent metal−oxo porphyrins are not usually described as strong bases, the overall negative charge of $[(Cz)Mn^{IV}(O)]^{-}$ compared to the neutral porphyrin analogue $[(porph)M^{IV}(O)]$, which arises from the trinegative corrolazine ligand, can help explain the enhanced basicity. The increased basicity in turn overcomes the low redox potential of the Mn^{V}−oxo complex (Step **I**, Scheme 2).

A similar argument regarding the basicity of Compound II in heme enzymes such as CPO and P450 has recently been offered.[25] The basicity of the thiolate-ligated ferryl intermediate found in cytochrome P450 (formally negatively charged, $[(Cys)(porph)Fe^{IV}{=}O]^{-}$) may contribute significantly to this enzyme's remarkable ability to oxidize hydrocarbons with inert C−H bonds. Although the basicity (i.e., the pK_a of $[(Cys)(porph)Fe^{IV}OH]$) for the intermediate in P450 is not known, this suggestion was based on the direct observation of a protonated ferryl intermediate ($Fe^{IV}OH$) in the closely related cysteinate-ligated active site of CPO. A pK_a of ≥ 8.2 was estimated for $[(CPO)Fe^{IV}OH]$. Assuming an H-atom abstraction mechanism for C−H oxidation by P450, a high basicity for $[(Cys)(porph)Fe^{IV}(O)]^{-}$ would allow for Compound I ($[(Cys)(porph)Fe^{V}(O)]$ or $(Cys)(porph^{+\bullet})Fe^{IV}(O)]$), the presumed reactive oxidant, to maintain a significantly lower redox potential then would otherwise be necessary. This idea is intriguing since, if correct, it helps to clarify the puzzling contradiction set up by the necessity of generating a very powerful oxidizing agent (Compound I) in the midst of a protein matrix susceptible to one-electron oxidation. In addition, it offers a rationale for the presence of the proximal Cys found in P450, which is to donate a third negative charge and increase the basicity of the ferryl intermediate.

The results presented here for **1** lend support to the former concepts. Complex **1** has a low redox potential and yet is still capable of performing hydrogen-atom abstractions. To our knowledge, this is the first concrete demonstration of H-atom abstraction by a high-valent metal−oxo porphyrinoid species with a low redox potential. The 'extra' negative charge provided by a corrolazine, as compared to a porphyrin, may be exerting a similar effect on the pK_a of the putative M^{IV}−OH intermediate as proposed for the negatively charged thiolate ligand in P450 and CPO.

Acknowledgment. We would like to thank the NSF (CHE0094095) for their support of this work and Prof. James Mayer and Prof. Michael Green for helpful discussions.

Supporting Information Available: Representative GC spectrum, representative kinetic fits. This material is available free of charge via the Internet at http://pubs.acs.org.

IC060491+